Magnetic Resonance Imaging in the Prognostic Evaluation of Patients with Pulmonary Arterial Hypertension

Andrew J. Swift[1,2], Dave Capener[1], Chris Johns[1], Neil Hamilton[3], Alex Rothman[1,2], Charlie Elliot[3], Robin Condliffe[3], Athanasios Charalampopoulos[3], Smitha Rajaram[4], Allan Lawrie[1,2], Michael J. Campbell[5], Jim M. Wild[1,2], and David G. Kiely[1,2,3]

[1]Department of Infection, Immunity and Cardiovascular Disease and [2]Insigneo Institute for *In Silico* Medicine, University of Sheffield, Sheffield, United Kingdom; [3]Sheffield Pulmonary Vascular Disease Unit, Royal Hallamshire Hospital and [4]Radiology Department, Sheffield Teaching Hospitals National Health Service Foundation Trust, Sheffield, United Kingdom; and [5]Scharr, Design, Trials & Statistics, Sheffield, United Kingdom

ORCID ID: 0000-0002-8772-409X (A.J.S.).

Abstract

Rationale: Prognostication is important when counseling patients and defining treatment strategies in pulmonary arterial hypertension (PAH).

Objectives: To determine the value of magnetic resonance imaging (MRI) metrics for prediction of mortality in PAH.

Methods: Consecutive patients with PAH undergoing MRI were identified from the ASPIRE (Assessing the Spectrum of Pulmonary Hypertension Identified at a Referral Centre) pulmonary hypertension registry.

Measurements and Main Results: During the follow-up period of 42 (range, 17–142) months 576 patients were studied and 221 (38%) died. A derivation cohort (n = 288; 115 deaths) and validation cohort (n = 288; 106 deaths) were identified. We used multivariate Cox regression and found two independent MRI predictors of death ($P < 0.01$): right ventricular end-systolic volume index adjusted for age and sex, and the relative area change of the pulmonary artery. A model of MRI and clinical data constructed from the derivation cohort predicted mortality in the validation cohort at 1 year (sensitivity, 70 [95% confidence interval (CI), 53–83]; specificity, 62 [95% CI, 62–68]; positive predictive value [PPV], 24 [95% CI, 16–32]; negative predictive value [NPV], 92 [95% CI, 87–96]) and at 3 years (sensitivity, 77 [95% CI, 67–85]; specificity, 73 [95% CI, 66–85]; PPV, 56 [95% CI, 47–65]; and NPV, 87 [95% CI, 81–92]). The model was more accurate in patients with idiopathic PAH at 3 years (sensitivity, 89 [95% CI, 65–84]; specificity, 76 [95% CI, 65–84]; PPV, 60 [95% CI, 46–74]; and NPV, 94 [95% CI, 85–98]).

Conclusions: MRI measurements reflecting right ventricular structure and stiffness of the proximal pulmonary vasculature are independent predictors of outcome in PAH. In combination with clinical data MRI has moderate prognostic accuracy in the evaluation of patients with PAH.

Keywords: magnetic resonance imaging; pulmonary arterial hypertension; prognosis; prognostic models

(Received in original form November 28, 2016; accepted in final form March 21, 2017)

Supported by the National Institute for Health Research (RP-R3-12-027), the Medical Research Council (MR/M008894/1) Pulmonary, Lung and Respiratory Imaging Sheffield, research fellowship CRTF MR/K002406/1 (A.R.), Bayer (D.C.), and the British Heart Foundation (FS/13/48/30453, A.L.).

Author Contributions: A.J.S. and D.G.K. conceived the idea for the study. A.J.S., J.M.W., A.R., M.J.C., and D.G.K. participated in the study design. A.J.S., D.C., C.J., and S.R. acquired the magnetic resonance imaging data. D.C., A.J.S., and J.M.W. developed and implemented the magnetic resonance imaging protocols used. Image analysis was performed by A.J.S., D.C., and S.R. A.C., M.J.C., J.M.W., A.R., C.E., R.C., A.L., N.H., and D.G.K. analyzed and interpreted the magnetic resonance data. A.J.S., S.R., A.R., C.E., R.C., A.L., N.H., D.C., J.M.W., M.J.C., and D.G.K. drafted the manuscript. All authors read and approved the final manuscript.

Correspondence and requests for reprints should be addressed to Andrew J. Swift, Ph.D., University of Sheffield, Academic Unit of Radiology, C Floor, Royal Hallamshire Hospital, Glossop Road, Sheffield S10 2JF, UK. E-mail: a.j.swift@shef.ac.uk

This article has an online supplement, which is accessible from this issue's table of contents at www.atsjournals.org

Am J Respir Crit Care Med Vol 196, Iss 2, pp 228–239, Jul 15, 2017

Originally Published in Press as DOI: 10.1164/rccm.201611-2365OC on March 22, 2017
Internet address: www.atsjournals.org

At a Glance Commentary

Scientific Knowledge on the Subject: Several candidate magnetic resonance imaging (MRI) metrics have been studied in the prognostic evaluation of patients with pulmonary arterial hypertension. However, the additive value of combining MRI metrics and accuracy of MRI for predicting mortality remains unclear.

What This Study Adds to the Field: MRI measurements of right ventricle volume and the stiffness of the proximal pulmonary vasculature are independent predictors of mortality in pulmonary arterial hypertension. A model of clinical data and MRI allows moderately accurate prediction of mortality in pulmonary arterial hypertension, and good accuracy in idiopathic pulmonary arterial hypertension.

Over the last two decades there has been significant progress in the treatment of pulmonary arterial hypertension (PAH) but despite this it remains a progressive life-shortening condition. Assessment of disease severity and estimating life expectancy is an important part of patient evaluation. It aids selection of treatment strategy, timing of transplantation, and counseling of patients (1).

Changes in the pulmonary vasculature in PAH cause an increase in right ventricular (RV) afterload, a reduction in cardiac output resulting in increasing breathlessness, and a fall in exercise capacity (2). Several measurements have been used to assess disease severity and estimate prognosis and include parameters reflecting symptomatic limitation (World Health Organization [WHO] function class [3]), impairment of RV function (elevated right atrial pressure [3–5], reduced cardiac output [4–6], and reduced mixed venous oxygen saturation [5]), and measurements of exercise capacity (6-minute-walk-test distance) (5, 6), and maximal oxygen uptake measured using cardiopulmonary exercise testing (7). In addition, multiparametric equations have been developed to improve the assessment of disease severity and aid prognostication (8, 9). All of these approaches are limited in part by inherent problems with reproducibility, subjective interpretation, and the invasive nature of investigations, such as cardiac catheterization.

Magnetic resonance imaging (MRI) provides accurate and reproducible information on cardiac morphology and function (10–12) and in addition also has sensitivity to changes in the pulmonary vasculature (13–16). Recently several studies have evaluated MRI as a tool to assess for the presence of PAH (14, 15, 17–21). In addition, studies have evaluated the prognostic value of MRI measurements; RV end-diastolic volume (RVEDV) and RV end-systolic volume (RVESV), RV ejection fraction (RVEF), and more recently RV-pulmonary artery (PA) coupling metrics and PA relative area change (13, 16, 22–25) have all been shown to have predictive value in patients with PAH. However, these studies have often been performed in relatively small numbers of patients and have concentrated on a limited number of parameters. The aim of this study was to investigate the prognostic value of combined cardiopulmonary MRI metrics in a large PAH registry.

Methods

Patients

Consecutive patients diagnosed with PAH at a pulmonary hypertension referral center, who underwent MRI, were identified from January 2008 to February 2015. Patients referred with suspected pulmonary hypertension underwent systematic evaluation as previously described in the ASPIRE (Assessing the Spectrum of Pulmonary Hypertension Identified at a Referral Centre) registry (26), including lung function, exercise testing, high-resolution computed tomography and computed tomography pulmonary angiography, MRI, and right heart catheterization. Treatment at the time of census or death was recorded as oral monotherapy (phosphodiesterase-5 inhibitor or endothelin receptor antagonist), oral combination therapy (phosphodiesterase-5 inhibitor and endothelin receptor antagonist), prostanoid therapy, or calcium channel blocker therapy. Ethical approval for this analysis of imaging techniques and routinely collected data was granted by our institutional review board (ref c06/Q2308/8).

MRI Acquisition

MRI was performed using an eight-channel cardiac coil on a GE HDx (GE Healthcare, Milwaukee, WI) whole-body scanner at 1.5 T. Short-axis cine images were acquired using a cardiac gated multislice balanced SSFP sequence (20 frames per cardiac cycle; slice thickness, 8 mm; field of view, 48; matrix, 256 × 256; BW, 125 kHz/pixel; TR/TE, 3.7/1.6 ms). A stack of images in the short-axis plane with slice thickness of 8 mm (2-mm inter-slice gap) were acquired fully covering both ventricles from base to apex. End-systole was considered to be the smallest cavity area. End-diastole was defined as the first cine phase of the R-wave triggered acquisition or largest volume. Through plane phase contrast imaging was performed orthogonal to the main pulmonary trunk. Phase contrast imaging parameters were as follows: repetition time, TR 5.6 ms; echo time, TE 2.7 ms; slice thickness, 10 mm; field of view, 48 cm, bandwidth, 62.5 kHz; matrix, 256 × 128; 20 reconstructed cardiac phases; and velocity encoding of flow, 150 cm/s. Patients were in the supine position with a surface coil and with retrospective ECG gating.

Image Analysis

Image analysis was performed on a GE Advantage Workstation 4.1 with the observer blinded to the patient clinical information, and cardiac catheter parameters. Right and left endocardial and epicardial surfaces were manually traced from the stack of short-axis cine images, using proprietary MR workstation software to obtain RVEDV and RVESV, and left ventricular (LV) end-diastolic volume (LVEDV) and LV end-systolic volume (LVESV). From end-diastolic and end-systolic volumes, RVEF and LV ejection fraction and RV and LV stroke volume (SV) were calculated. With the exception of RVEF and LV ejection fraction, these measurements were indexed for body surface area. Based on previous work, SV was considered to be the most accurate from LV volumetry (27) and was used for MRI estimation of RV–PA coupling. For calculation of ventricular mass the interventricular septum was considered as part of the LV. RV end-diastolic mass (RV mass) and LV end-diastolic mass were derived (LV mass). Ventricular mass index was defined

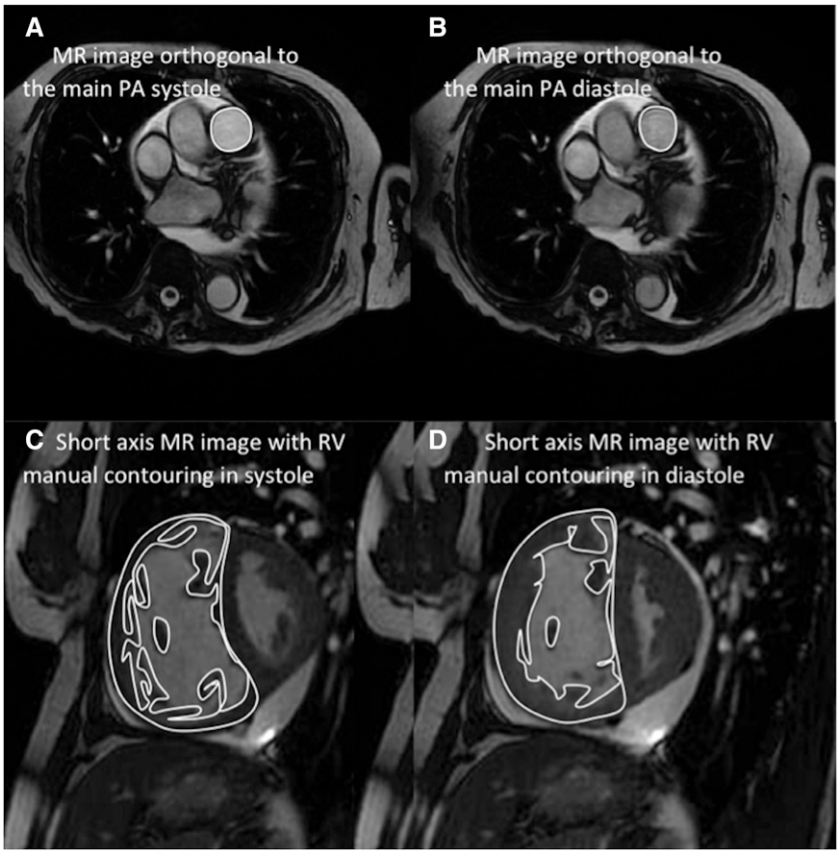

Figure 1. Images detailing pulmonary artery (PA) size and relative area change analysis. Maximal PA area (*A*) and minimal PA area (*B*), and right ventricular volume and mass calculation from end-diastolic images (*C*) and end-systolic images (*D*). MR = magnetic resonance; RV = right ventricle.

as RV mass divided by LV mass, as previously described (18). Maximal and minimal PA areas were measured, and relative area change was defined by the following equation: relative area change = (maximum area − minimum area)/minimum area (Figure 1) (14, 28).

Right Heart Catheterization and Clinical Assessment

Right heart catheterization was performed using a balloon-tipped 7.5F thermodilution catheter (Becton-Dickinson, Franklin Lakes, NJ). Right heart catheterization was usually performed via the internal jugular vein using a Swan-Ganz catheter. Features at right heart catheterization required to define PAH were mean PA pressure (mPAP) greater than or equal to 25 mm Hg at rest with a pulmonary arterial wedge pressure (PAWP) of less than or equal to 15 mm Hg (29). Pulmonary vascular resistance (PVR) was determined as follows: PVR = (mPAP − PAWP)/cardiac output. Cardiac output was measured by thermodilution technique. Diagnostic classification of the form of PAH was made using standard criteria after multiprofessional assessment (26). To be included in the study patients were also required to have received treatment with PAH therapy during the study period.

Coupling Measurements

As previously described, RV elastance (Ees) was estimated as mPAP divided by RVESV index (30). Pulmonary arterial elastance (Ea) was estimated using mPAP − PAWP divided by SV index. Therefore, Ees/Ea by a combined right heart catheterization and MRI approach was defined as follows: (mPAP/RVESV index)/[(mPAP − PAWP)/SV index]. MRI estimated Ees/Ea was defined by SV/RVESV (24, 30–32). Table 1 summarizes the coupling measurements and pulmonary arterial relative area change metrics.

Statistics

The interval from evaluation with MRI until all-cause death or July 15, 2016, was regarded as the follow-up period. Individual analyses of mortality at 1 and 3 years were also performed. Log-log plots were produced for each variable to assess proportional hazards; continuous variables

Table 1. Definition of Pulmonary Arterial and Right Ventricular Elastance, Coupling Measurements, and Pulmonary Artery Stiffness Metrics

Key Metrics	Measurement Description	Equation
Ea, mm Hg/ml/m^2	Arterial elastance	(mPAP − PAWP)/stroke volume index
Ees, mm Hg/ml/m^2	RV elastance	mPAP/RV end-systolic volume index
Ees/Ea, ratio	PA–RV coupling metric	(mPAP/RV end-systolic volume)/[(mPAP − PAWP)/stroke volume]
MRI Ees/Ea, ratio	Noninvasive PA–RV coupling metric	Stroke volume/RV end-systolic volume
PA relative area change, %	Noninvasive measurement of PA stiffness	(Maximal pulmonary arterial area − minimal pulmonary arterial area)/minimal pulmonary arterial area
Distensibility, %/PP	Measurement of PA stiffness	PA relative area change/pulse pressure

Definition of abbreviations: Ea = arterial load; Ees = RV elastance; mPAP = mean pulmonary artery pressure; MRI = magnetic resonance imaging; PA = pulmonary artery; PAWP = pulmonary arterial wedge pressure; PP = pulse pressure; RV = right ventricular.

were dichotomized for this analysis by median values. Cardiovascular magnetic resonance (CMR) volumetric measurements indexed for body surface area were corrected for age and sex and presented as percentage predicted as per prior data by Maceira and coworkers (33) and Kawut and coworkers (34). The prognostic value of MRI-derived biventricular volume, mass and function, PA measurements, mPAP, mean right atrial pressure, cardiac index, PVR, mixed venous oxygen saturation ($S\bar{v}_{O_2}$), RV–PA coupling indices, and patient age, sex, and WHO functional class were assessed using univariate Cox proportional hazards regression analysis. Variable scaling was performed to allow direct comparison of hazard ratios of all continuous variables by dividing individual values by the SD of the variable. Multivariate analysis with a forward stepwise approach was performed for demographic, CMR, and right heart catheterization data significant at univariate analysis ($P < 0.2$). Highly correlated variables ($r > 0.8$) that were significant at univariate Cox analysis were entered separately into the model. If noninvasive and invasive variables metrics were highly correlated, the noninvasive metrics was entered into the multivariate analysis if both metrics were significant at univariate analysis.

Idiopathic PAH (IPAH), the largest diagnostic population, was used as the

Table 2. Univariate Cox Proportional Hazards Regression Analysis Showing Prognostic Significance of Demographic, Right Heart Catheterization, and MRI Data for the Full Cohort

	Univariate Hazard Ratio	Scaled Univariate Hazard Ratio	*P* Value	N
Demographics				
Age (dichotomized <50 and ⩾50 yr)	4.092 (2.697–6.208)		<0.0001*	576
Sex, female, %	0.794 (0.600–1.049)		0.105	576
WHO function class				
I and II vs. III and IV	1.876 (1.126–3.125)		0.016	
I–III vs. IV	2.636 (1.912–3.634)		<0.0001*	
IPAH	0.873 (0.669–1.140)		0.319	
CTD	1.572 (1.202–2.056)		0.001*	
Congenital	0.389 (0.212–0.713)		0.002	
Other	0.971 (0.625–1.509)		0.897	
PAH therapy				
Monotherapy oral	1.658 (1.281–2.239)		<0.0001	576
Combination oral	0.684 (0.524–0.892)		0.005	576
Prostanoid	0.946 (0.679–1.317)		0.742	576
RHC				
mPAP, mm Hg	0.997 (0.987–1.008)	0.968 (0.842–1.112)	0.643	447
mRAP, mm Hg	1.019 (0.994–1.045)	1.112 (0.967–1.279)	0.137	443
PAWP, mm Hg	0.978 (0.938–1.019)	0.926 (0.804–1.067)	0.291	440
$S\bar{v}_{O_2}$, %	0.969 (0.955–0.983)	0.738 (0.644–0.847)	<0.0001*	446
CI, L/min/m^2	0.826 (0.698–0.979)	0.840 (0.720–0.981)	0.027	446
PVRI, dyn/s/cm^3	1.008 (0.991–1.025)	1.065 (0.931–1.218)	0.359	440
Cardiac MR indices				
RVEDVI %pred	1.005 (1.002–1.007)	1.244 (1.107–1.399)	<0.0001*	576
RVESVI %pred	1.003 (1.002–1.004)	1.403 (1.256–1.567)	<0.0001*	576
RVEF %pred	0.987 (0.981–0.993)	0.754 (0.662–0.860)	<0.0001*	576
RVSVI %pred	0.999 (0.995–1.003)	0.956 (0.838–1.091)	0.506	576
LVEDVI %pred	0.990 (0.984–0.996)	0.998 (0.996–0.999)	0.002	576
LVESVI %pred	0.998 (0.994–1.002)	0.999 (0.998–1.001)	0.359	576
LVEF %pred	0.993 (0.985–1.001)	0.898 (0.790–1.022)	0.103	576
LVSVI %pred	0.990 (0.983–0.996)	0.744 (0.619–0.896)	0.002	563
RVEDMI %pred	1.001 (1.000–1.002)	1.149 (1.009–1.308)	0.036	563
PA forward flow index, L/min/m^2	0.851 (0.761–0.951)	0.797 (0.682–0.932)	0.004	556
PA stiffness metrics				
PA relative area change	0.951 (0.932–0.971)	0.672 (0.569–0.794)	<0.0001*	557
PA distensibility	0.134 (0.045–0.401)	0.536 (0.381–0.754)	<0.0001*	447
RV–PA coupling metrics				
Ea, mm Hg/ml/m^2	1.036 (0.942–1.140)	1.051 (0.920–1.201)	0.462	442
Ees, mm Hg/ml/m^2	0.921 (0.831–1.020)	0.793 (0.667–0.944)	0.112	447
Ees/Ea ratio	0.549 (0.401–0.753)	0.777 (0.673–0.896)	0.001*	442
MRI Ees /Ea ratio	0.525 (0.375–0.736)	0.739 (0.621–0.866)	<0.0001*	576

Definition of abbreviations: CI = cardiac index; CTD = connective tissue disease; Ea = arterial load; Ees = RV elastance; IPAH = idiopathic pulmonary arterial hypertension; LVEDVI = left ventricular end-diastolic volume index; LVEF = left ventricular ejection fraction; LVESVI = left ventricular end-systolic volume index; LVSVI = left ventricular stroke volume index; mPAP = mean pulmonary artery pressure; mRAP = mean right atrial pressure; MR = magnetic resonance; MRI = MR imaging; PA = pulmonary artery; PAH = pulmonary arterial hypertension; PAWP = pulmonary arterial wedge pressure; PVRI = pulmonary vascular resistance index; RHC = right heart catheterization; RV = right ventricular; RVEDMI = right ventricular end-diastolic mass index; RVEDVI = right ventricular end-diastolic volume index; RVEF = right ventricular ejection fraction; RVESVI = right ventricular end-systolic volume index; RVSVI = right ventricular stroke volume index; $S\bar{v}_{O_2}$ = mixed venous oxygen saturation; WHO = World Health Organization.
N = 576 (211 deaths). Data in parentheses are 95% confidence intervals.
*Significant after Bonferonni correction.

reference category for multivariate analysis and combination therapy, being the largest therapy group, was used as the reference category for multivariate analysis. Derivation and validation cohorts were constructed to develop models encompassing MRI data alone and MRI and clinical data combined. Patients were assigned a study number based on the date of the MRI study, with the first patient scanned assigned a number of n = 1 and the last patient scanned assigned a number of n = 576. Those with an odd number were assigned to the derivation cohort and those with an even number were assigned to the validation cohort. In the derivation cohort variables significant at a univariate *P* less than 0.2 were entered into a multivariate Cox proportional hazards regression model. The model was used to predict outcome in the validation cohort.

Kaplan-Meier plots were constructed to illustrate the prognostic value of MRI volumetric measurements using median threshold values. Groups were compared using the log-rank (Mantel-Cox) test. Receiver operating characteristic (ROC) analysis was used to assess prognostic significance of candidate predictors of mortality with area under the curve (AUC) data presented for mortality at 1 and 3 years. The sensitivity, specificity, positive predictive value (PPV), and negative predictive value (NPV) were derived from the 2 × 2 prediction table. For ROC comparison we have used a nonparametric method analogous to the Wilcoxon/Mann-Whitney test as previously described (35). The derivation cohort was used to develop predictive thresholds for CMR parameters. In addition, Bonferroni correction was performed on the univariate candidate predictors of mortality (n = 32) and variables that reached statistical significance *P* less than 0.0016 are shown in Table 2. Interobserver and intraobserver reproducibility was tested in 30 randomly selected cases using intraclass correlation coefficient. Statistical analysis was performed using SPSS 19 (SPSS, Chicago, IL) and for presentation of the data GraphPad Prism 6.04 (GraphPad Software, San Diego, CA) software was used. A *P* value less than 0.05 was considered statistically significant.

Results

A total of 576 patients with PAH were identified. A total of 398 patients were incident and treatment naive, and 178 patients were prevalent patients with PAH on PAH therapy (Figure 2). Table 3 shows the demographic, MRI, and right heart catheterization data for (*1*) the total study cohort, (*2*) incident patients with PAH who were treatment naive, and (*3*) prevalent patients with PAH on PAH treatment. The study group included 260 patients with IPAH; 195 patients with PAH associated with connective tissue disease (CTD); 63 patients with congenital heart disease; and 58 patients with PAH associated with HIV, portal hypertension, or drugs and toxins. Table 4 summarizes the baseline characteristics of incident treatment-naive patients with IPAH and PAH-CTD.

Survival Analyses

Full cohort. During the follow-up period 221 patients (38%) died (mean follow-up, 42 mo; range, 17–142). Table 2 presents the univariate Cox proportional hazards regression analysis data for demographic, hemodynamic, and MRI data. MRI measures of RV size and function (RVESV %pred [$P < 0.0001$], RVEF %pred [$P < 0.0001$], and invasive and noninvasive MRI-derived Ees/Ea [$P < 0.001$]) predicted mortality at univariate Cox regression analysis. Both PA relative area change and pulmonary arterial distensibility ($P < 0.0001$) predicted mortality at univariate Cox regression analysis after Bonferroni correction. Age greater than 50, WHO functional class IV, and $S\bar{v}_{O_2}$ (all $P < 0.0001$) were also predictive of mortality, all remaining significant after Bonferroni correction. PA relative area change and distensibility were highly correlated ($r = 0.88$; $P < 0.0001$). In the multivariate analysis increased RVESVI %pred ($P = 0.005$) reduced PA relative area change ($P = 0.008$), age greater than 50 ($P < 0.0001$), the presence of CTD ($P = 0.039$), and decreased $S\bar{v}_{O_2}$ ($P = 0.006$) and oral monotheray as compared with combination oral therapy ($P = 0.006$) were associated with worse outcome. Figure 3 shows Kaplan-Meier plots for RVESVI % pred and PA relative area change above and below median thresholds.

Incident and prevalent cases. Incident treatment-naive patients were older ($P < 0.0001$) (Table 3) and had worse outcome at Cox regression analysis (hazard ratio, 2.338; 95% confidence interval [CI], 1.603–3.408; $P < 0.0001$) than prevalent patients with PAH on therapy. Incident patients had more severe hemodynamic impairment with lower $S\bar{v}_{O_2}$ ($P = 0.003$) and cardiac index ($P < 0.0001$) and on MRI had evidence of more severe disease with higher RVESVI %pred ($P < 0.0001$) and lower RVEF %pred, LVEDV %pred ($P < 0.0001$), and PA relative area change ($P < 0.0001$) (Table 3). In the multivariate Cox regression analysis of incident patients the same predictors were significant as in the full cohort inclusive of incident and prevalent cases. Age greater than 50, lower $S\bar{v}_{O_2}$, and lower PA relative area change were independent indicators of adverse outcome; lower RVESVI %pred and combination oral therapy predicted improved survival (Table 5).

Subgroup analysis: IPAH and PAH-CTD. In incident treatment-naive patients with IPAH there were several independent variables that predicted outcome at

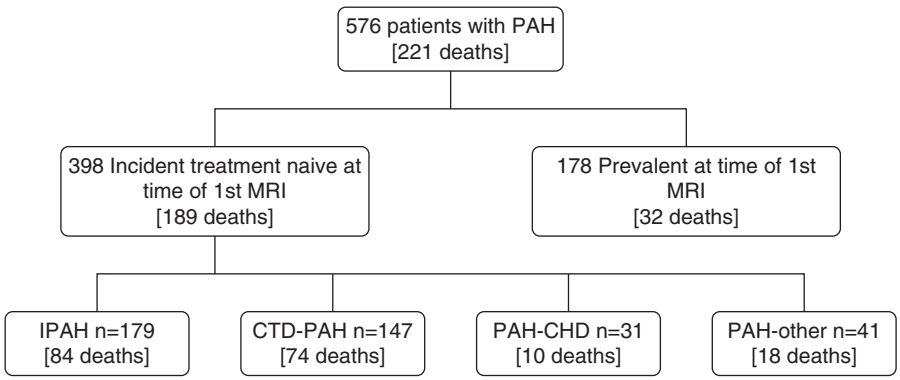

Figure 2. Study flow diagram. CHD = congenital heart disease; CTD = connective tissue disease; IPAH = idiopathic pulmonary arterial hypertension; MRI = magnetic resonance imaging; PAH = pulmonary arterial hypertension.

Table 3. Baseline Demographic, MRI, and Right Heart Catheterization Data

Demographics	All Patients (*n* = 576)	Incident Patients (*n* = 398)	Prevalent Patients (*n* = 178)	*P* Value	N
Age, yr	57 (16)	60 (15)	52 (17)	<0.0001	576
Sex M/F, n (male %)	182/394 (46)	132/266 (50)	50/128 (39)	0.223	576
WHO functional class, n					
I	5	2	3		
II	50	32	17		
III	451	308	141		
IV	70	56	14		
Subgroup, n					
IPAH	260	179	80	0.946	
CTD	195	147	48	0.022	
Congenital	63	31	32	<0.0001	
Other (portal, HIV, and drugs)	58	41	18	0.883	
PAH therapy, n					
Monotherapy oral	155	126	29	<0.0001	576
Combination oral	308	205	104	0.138	576
Prostanoid	107	62	45	0.005	576
RHC					
mPAP, mm Hg	48 (13)	48 (13)	45 (14)	0.090	447
mRAP, mm Hg	10 (6)	10 (3)	10 (5)	0.369	443
PAWP, mm Hg	10 (3)	10 (3)	11 (3)	0.046	440
$S\bar{v}_{O_2}$, %	64 (10)	63 (9)	67 (10)	0.003	446
CI, L/min/m^2	2.8 (0.9)	2.7 (0.8)	3.3 (1.1)	<0.0001	446
PVRI, Wood units · m^2	16 (8.1)	15.7 (7.9)	14.0 (9.5)	0.206	440
Cardiac MR indices					
RVEDVI, ml/m^2	94 (35)	94 (33)	94 (40)	0.978	576
RVEDVI %pred	128 (47)	129 (45)	124 (52)	0.233	576
RVESVI, ml/m^2	59 (29)	62 (28)	54 (30)	0.005	576
RVESVI %pred	246 (125)	262 (126)	210 (117)	<0.0001	576
RVEF %	39 (14)	36 (14)	44 (13)	<0.0001	576
RVEF %pred	58 (22)	54 (21)	67 (20)	<0.0001	576
RVSVI, ml/m^2	35 (16)	33 (14)	40 (19)	<0.0001	576
RVSVI %pred	71 (33)	67 (30)	20 (19)	<0.0001	576
LVEDVI, ml/m^2	54 (19)	50 (16)	61 (23)	<0.0001	576
LVEDVI %pred	69 (24)	66 (21)	79 (30)	<0.0001	576
LVESVI, ml/m^2	18 (9)	17 (8)	20 (11)	0.001	576
LVESVI %pred	73 (38)	70 (35)	79 (46)	0.049	576
LVEF %	67 (11)	66 (11)	68 (9)	0.036	576
LVEF %pred	98 (15)	97 (16)	101 (14)	0.008	576
LVSVI, ml/m^2	26 (14)	23 (12)	12 (16)	<00001	576
LVSVI %pred	52 (28)	47 (24)	65 (32)	<0.0001	576
RVEDMI	35 (20)	36 (20)	34 (21)	0.330	563
RVEDMI %pred	124 (70)	127 (70)	114 (70)	0.120	563
PA forward flow index, L/min/m^2	3.2 (1.4)	3.0 (1.3)	3.6 (1.5)	<0.0001	556
PA stiffness metrics					
PA relative area change	12 (8)	11 (7)	14 (9)	<0.0001	557
PA distensibility	0.28 (0.31)	0.25 (0.30)	0.37 (0.31)	0.003	447
RV–PA coupling metrics					
Ea, mm Hg/ml/m^2	2.0 (1.4)	2.2 (1.4)	1.4 (1.2)	<0.0001	442
Ees, mm Hg/ml/m^2	0.95 (0.246)	0.9 (0.5)	1.0 (0.5)	0.024	447
Ees/Ea ratio	0.80 (0.83)	0.7 (0.7)	1.3 (1.2)	<0.0001	442
MRI Ees/Ea ratio	0.74 (0.47)	0.7 (0.4)	0.9 (0.5)	<0.0001	576

Definition of abbreviations: CI = cardiac index; CTD = connective tissue disease; Ea = arterial load; Ees = RV elastance; IPAH = idiopathic pulmonary arterial hypertension; LVEDVI = left ventricular end-diastolic volume index; LVEF = left ventricular ejection fraction; LVESVI = left ventricular end-systolic volume index; LVSVI = left ventricular stroke volume index; mPAP = mean pulmonary artery pressure; mRAP = mean right atrial pressure; MR = magnetic resonance; MRI = MR imaging; PA = pulmonary artery; PAH = pulmonary arterial hypertension; PAWP = pulmonary arterial wedge pressure; PVRI = pulmonary vascular resistance index; RHC = right heart catheterization; RV = right ventricular; RVEDMI = right ventricular end-diastolic mass index; RVEDVI = right ventricular end-diastolic volume index; RVEF = right ventricular ejection fraction; RVESVI = right ventricular end-systolic volume index; RVSVI = right ventricular stroke volume index; $S\bar{v}_{O_2}$ = mixed venous oxygen saturation; WHO = World Health Organization.
Values are presented as mean (SD) unless otherwise stated.

Table 4. Demographics and Comparison of Incident Treatment-Naive Patients with IPAH and PAH-CTD

Demographics	IPAH (*n* = *179*)	PAH-CTD (*n* = *147*)	*P* Value	N
Age, yr	60 (16)	63 (13)	0.093	326
Sex M/F, n	73/106	31/116	<0.0001	326
WHO functional class, n				
I	0	1		
II	14	9		
III	128	121		
IV	137	16		
PAH therapy, n				
Monotherapy oral	61	49	0.888	326
Combination oral	82	82	0.074	326
Prostanoid	36	16	0.024	326
RHC				
mPAP, mm Hg	52 (11)	43 (12)	<0.0001	305
mRAP, mm Hg	11 (5)	10 (6)	0.061	303
PAWP, mm Hg	10 (3)	10 (3)	0.207	302
$S\bar{v}_{O_2}$, %	61 (9)	65 (8)	<0.0001	298
CI, L/min/m^2	2.5 (0.8)	2.9 (0.8)	<0.0001	304
PVRI, Wood units · m^2	18.1 (7.5)	13.1 (8.2)	<0.0001	299
Cardiac MR indices				
RVEDVI %pred	134 (43)	117 (37)	<0.0001	326
RVESVI %pred	286 (126)	235 (116)	<0.0001	326
RVEF %pred	48 (18)	57 (22)	<0.0001	326
RVSVI %pred	63 (19)	64 (23)	0.758	326
LVEDVI %pred	63 (19)	67 (18)	0.095	326
LVESVI %pred	72 (38)	67 (18)	0.136	326
LVEF %pred	93 (16)	101 (15)	<0.0001	326
LVSVI %pred	41 (21)	51 (25)	<0.0001	326
RVEDMI %pred	215 (119)	166 (93)	<0.0001	326
PA forward flow index, L/min/m^2	2.6 (1.0)	3.0 (0.9)	<0.0001	326
PA stiffness metrics				
PA relative area change	10 (6)	11 (8)	0.089	309
PA distensibility	0.18 (0.15)	0.31 (0.35)	0.001	300
RV PA coupling metrics				
Ea, mm Hg/ml/m^2	1.8 (1.9)	1.3 (1.3)	0.003	300
Ees, mm Hg/ml/m^2	0.89 (0.34)	0.98 (0.43)	0.047	305
Ees/Ea ratio	0.45 (0.34)	0.95 (0.84)	<0.0001	300
MRI Ees/Ea ratio	0.54 (0.31)	0.75 (0.47)	<0.0001	326

Definition of abbreviations: CI = cardiac index; CTD = connective tissue disease; Ea = arterial load; Ees = RV elastance; IPAH = idiopathic pulmonary arterial hypertension; LVEDVI = left ventricular end-diastolic volume index; LVEF = left ventricular ejection fraction; LVESVI = left ventricular end-systolic volume index; LVSVI = left ventricular stroke volume index; mPAP = mean pulmonary artery pressure; mRAP = mean right atrial pressure; MR = magnetic resonance; MRI = MR imaging; PA = pulmonary artery; PAH = pulmonary arterial hypertension; PAWP = pulmonary arterial wedge pressure; PVRI = pulmonary vascular resistance index; RHC = right heart catheterization; RV = right ventricular; RVEDMI = right ventricular end-diastolic mass index; RVEDVI = right ventricular end-diastolic volume index; RVEF = right ventricular ejection fraction; RVESVI = right ventricular end-systolic volume index; RVSVI = right ventricular stroke volume index; $S\bar{v}_{O_2}$ = mixed venous oxygen saturation; WHO = World Health Organization.
Values are presented as mean (SD) unless otherwise stated.

multivariate analysis: RVESVI %pred (P = 0.001), Ees (P = 0.035), low $S\bar{v}_{O_2}$ (P = 0.002), age greater than 50 (P = 0.010), and male sex (P = 0.029) (Table 5). At ROC analysis, RVESVI %pred was predictive of mortality in patients with IPAH at 1 and 3 years (AUC, 0.716 and 0.735, respectively).

In incident treatment-naive patients with PAH-CTD, PA stiffness measured by PA relative area change (P = 0.003) and Ees/Ea (combined invasive/noninvasive metric; P = 0.010) and treatment (oral monotherapy as compared with combination therapy; P = 0.019) were independent predictors of outcome at multivariate analysis (Table 5). In PAH-CTD PA relative area change was predictive of mortality at 1 and 3 years (AUC of 0.640 and AUC of 0.696, respectively).

Prognostic model and validation. A derivation cohort (n = 288; 115 deaths) and validation cohort (n = 288; 106 deaths) were identified. There was no significant difference in age, sex, WHO functional class, MRI data, right heart catheter hemodynamics, time to death or census, or the proportion of CTD, IPAH, or congenital heart disease or male patients between the validation and derivation cohorts (all $P >$ 0.05). In the derivation cohort the following model was derived from multivariate Cox regression analysis of MRI and clinical data:

Prognostic score = (RVESVI (%pred) × 0.002) − (PA relative area change × 0.026) + (WHO function class × 0.458) + (Age × 0.031) − (male = 0.488 or female = 0.976) + (0.304 if CTD).

In the validation cohort the model showed the following accuracy: AUC of 0.741 and AUC of 0.815 at 1 and 3 years. A model based on MRI parameters alone (RVESVI %pred × 0.003 − PA relative area change × 0.060) demonstrated the following prognostic accuracy at 3 years in all

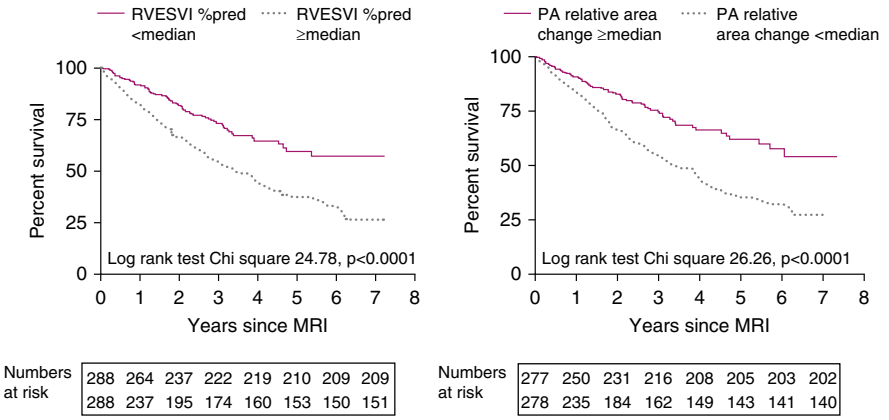

Figure 3. Kaplan-Meier survival curves showing the outcome of right ventricular end-systolic volume % predicted (*left*) and pulmonary artery (PA) relative area change (*right*). Numbers at risk are presented below each plot. MRI = magnetic resonance imaging; RVESVI = right ventricular end-systolic volume index.

PAH (AUC, 0.741), in IPAH (AUC, 0.820) (Figure 4) and in PAH-CTD (AUC, 0.690).

Optimal thresholds at ROC analysis were identified in the derivation cohort for RVESVI %pred: 180%, the MRI model: 0.13 units and the model including MRI and clinical data: 2.9 units. In the validation cohort at 1 year the MRI and clinical data model predicted mortality; sensitivity of 70 (95% CI, 53–83), specificity of 62 (95% CI, 62–68), PPV of 24 (95% CI, 16–32), and NPV of 92 (95% CI, 87–96), respectively. Table 6 presents the sensitivity, specificity, PPV, and NPV data for these optimal thresholds for 3-year mortality. There was no significant difference at ROC analysis for predicting mortality between current methods of correcting MRI data for age, sex, and body size (Maceira and coworkers [33] and Kawut and coworkers [34]); RVEDV ($P = 0.955$); RVEF ($P = 0.236$); and RVEDM ($P = 0.635$).

Reproducibility of MR indices. Excellent interobserver reproducibility was identified for RVEDV and RVESV measurements; with high intraclass correlation coefficients (ICC) demonstrated, 0.959 and 0.991, respectively. The agreement was found to be marginally weaker for RVEF and SV measurements 0.957 and 0.928, respectively. Excellent interobserver reproducibility was identified for LV volume and LV function ICC 0.953–0.988. High intraobserver agreement for RV volume and function measurements was shown (ICC 0.940–0.996), and similarly high intraobserver agreement was found for LV volume measurements (ICC 0.973–0.986). MRI estimated Ees/Ea had high interobserver and intraobserver reproducibility, ICC 0.938 and 0.977, respectively. PA relative area change had high interobserver and intraobserver reproducibility, ICC 0.891 and ICC 0.900, respectively.

Table 5. Multivariate Analyses Showing Independent Predictors of Outcome in the Whole PAH Cohort, All Incident Patients with PAH, and Incident Patients with IPAH and CTD

	Multivariate Hazard Ratio	*P* Value
Full cohort		
Age >50 yr	2.787 (1.691–4.592)	<0.0001
Presence of CTD	1.421 (1.017–1.984)	0.039
Monotherapy vs. combination therapy	1.700 (1.200–2.409)	0.003
$S\bar{v}_{O_2}$ (scaled)	0.792 (0.672–0.934)	0.006
RVESV %pred (scaled)	1.217 (1.061–1.539)	0.005
PA RAC (scaled)	0.762 (0.623–0.932)	0.008
Incident cases		
Age >50 yr	2.324 (1.380–3.915)	0.002
Monotherapy vs. combination therapy	1.571 (1.087–2.270)	0.016
$S\bar{v}_{O_2}$ (scaled)	0.790 (0.661–0.944)	0.009
RVESV %pred (scaled)	1.186 (1.015–1.385)	0.032
PA RAC (scaled)	0.741 (0.589–0.932)	0.010
IPAH		
Age >50 yr	2.837 (1.200–6.708)	0.010
Female	0.583 (0.360–0.945)	0.029
$S\bar{v}_{O_2}$ (scaled)	0.652 (0.495–0.858)	0.002
Ees (scaled)	0.781 (0.621–0.983)	0.035
RVESV %pred (scaled)	1.408 (1.147–1.729)	0.001
CTD-PAH		
Monotherapy vs combination therapy	2.182 (1.282–3.714)	0.004
Ees/Ea (scaled)	0.757 (0.642–0.892)	0.001
PA RAC (scaled)	0.653 (0.496–0.859)	0.002

Definition of abbreviations: CTD = connective tissue disease; Ea = arterial load; Ees = RV elastance; IPAH = idiopathic pulmonary arterial hypertension; PA RAC = pulmonary artery relative area change; PAH = pulmonary arterial hypertension; RVESV = right ventricular end-systolic volume; $S\bar{v}_{O_2}$ = mixed venous oxygen saturation.
Data in parentheses are 95% confidence intervals.

Discussion

This study confirms the independent prognostic value of MRI measurements reflecting RV volume and stiffness of the proximal pulmonary vasculature in a large cohort of patients with PAH. In addition, a model combining MRI measurements of RVESV (%pred) and PA relative area change in combination with clinical data (age, sex, WHO function class, and the presence or absence of an underlying CTD), improves prognostication in PAH.

Many indices of RV size and function have been proposed as prognostic markers in the patients with pulmonary hypertension; however, previous studies have often been performed in comparatively small cohorts of patients. Given the large number of patients in the current study and the number of deaths during the follow-up period it has provided an opportunity to assess the relative value of a number of candidate MRI prognostic

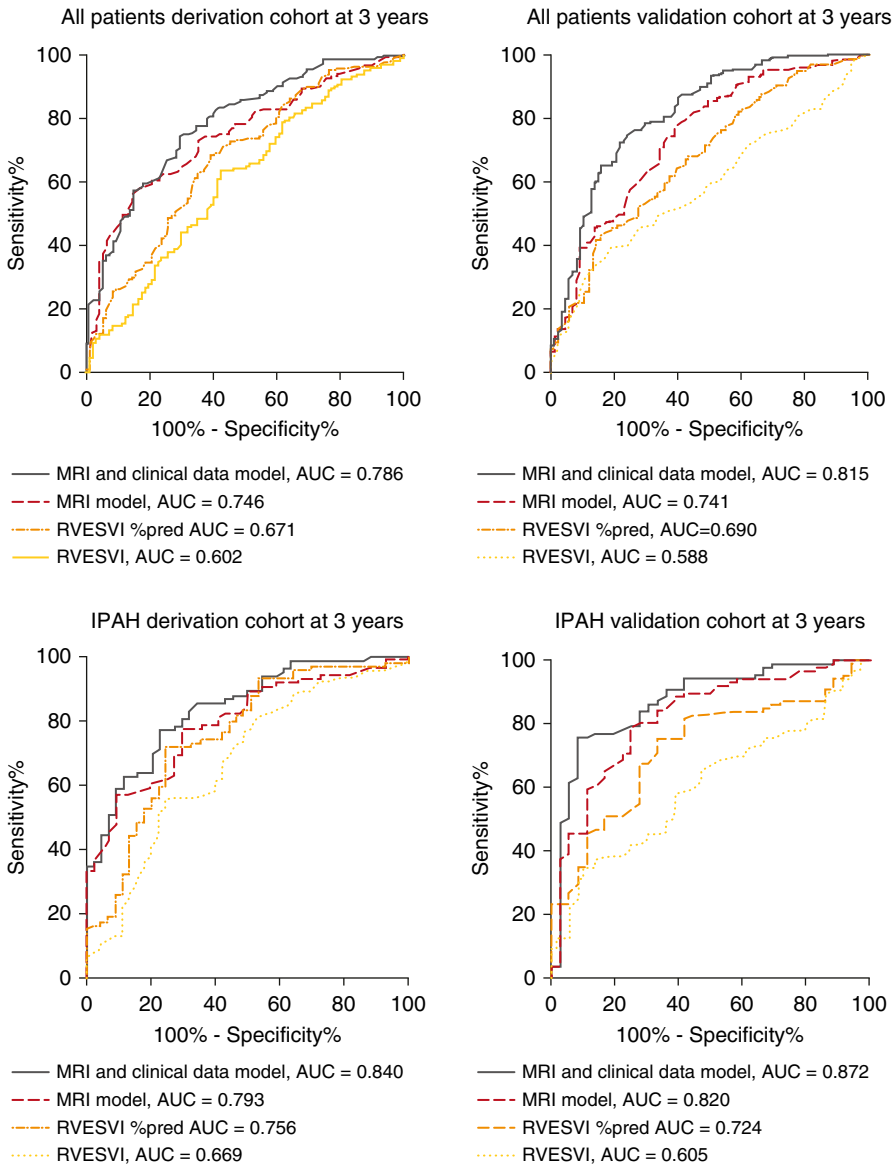

Figure 4. Receiver operating curves showing important predictors of mortality in all patients with pulmonary arterial hypertension in the derivation cohort (*top left*) and validation cohort (*top right*), and patients with idiopathic pulmonary arterial hypertension in the derivation cohort (*bottom left*) and validation cohort (*bottom right*). AUC = area under the curve; IPAH = idiopathic pulmonary arterial hypertension; MRI = magnetic resonance imaging; RVESVI = right ventricular end-systolic volume index.

markers. This study confirms the prognostic value of RV volumes and ejection fraction measured at MRI shown in previous studies (23, 25). Although in clinical practice physicians have traditionally favored single measurements, such as RVEF, this study demonstrates the added prognostic value of combining a measure of the RV (RVESVI %pred) and a measure of changes in the proximal pulmonary vasculature (PA relative area change).

A criticism of relatively simple measures thought to reflect RV function, such as volumes and ejection fraction, is that these metrics are not load independent (36). Recently more complex measurements reflecting RV–PA coupling, described by the simultaneous relationship between two load independent metrics, RV contractility (Ees) and afterload (Ea) (36), have been proposed as superior to volumetric measurements. Previous work has shown that parameters, such as Ees and Ea, can be estimated from standard data collected from right heart catheterization and MRI (30), rather than using conductance catheters not typically used in routine clinical practice. In the current study, in patients with PAH-CTD combined MRI and right heart catheterization Ees/Ea was independently predictive of mortality although not found to be independently prognostic in the full cohort. In addition, a completely noninvasive MR-based approach and techniques using gated blood pool scintingraphy can yield measures of RV–PA coupling acknowledging previously described limitations (24, 30–32, 37). A recent study has shown the superior prognostic significance of an MRI-derived estimate of RV-arterial coupling Ees/Ea over other invasive and noninvasive measures of RV function (24). However, no additional prognostic value of an MRI-only measurement of RV–PA coupling over volumetric indices was demonstrated in the present study.

Independent prognostic markers differed between IPAH and PAH-CTD. In IPAH measures of RV size and function, RVESV % predicted, and Ees were independently prognostic, in addition to age, sex, and $S\bar{v}_{O_2}$. Whereas, independent prognostic markers in PAH-CTD were pulmonary arterial relative area change and Ees/Ea (combined invasive/MRI). These differences are likely to reflect the individual pathophysiology and therapy responsiveness of PAH subgroups and reinforces that subgroups have differing prognostic markers. In contrast, to a previous study by Tedford and coworkers (38) we found patients with PAH associated with CTD had higher contractive RV function (Ees) relative to afterload (Ea). We estimated coupling indices using hemodynamic data collected from standard right heart catheterization studies and MRI and did not perform dedicated pressure-volume studies. There are assumptions made using simplified measures of coupling and differences in the populations in these two studies may explain these disparities. Further research studying RV adaption to elevated afterload in these subgroups is warranted.

PA relative area change was found to be an independent prognostic marker in the full cohort, and our data suggest that the stiffness of the pulmonary vasculature has independent prognostic value in addition to baseline measurements reflecting RV function. The present study shows comparable univariate prognostic value of

Table 6. Prognostic Accuracy of MRI Metrics and Models in the Validation Cohort for Predicting Mortality at 3 Years

	Sens	Spec	PPV	NPV	LHR	*P* Value
Full cohort, prognostic model 3 yr						
RV end-systolic volume %pred	61 (50–71)	63 (56–70)	43 (34–52)	78 (71–84)	1.64	0.0002
MRI model	71 (61–80)	63 (55–70)	47 (38–55)	83 (75–88)	1.91	<0.0001
MRI and demographic model	77 (67–85)	73 (66–85)	56 (47–65)	87 (81–92)	2.78	<0.0001
Treatment-naive PAH, prognostic model 3 yr						
RV end-systolic volume %pred	59 (49–69)	62 (52–72)	60 (49–70)	61 (51–71)	1.56	0.0041
MRI model	70 (59–80)	56 (46–65)	52 (43–63)	73 (61–82)	1.57	0.0001
MRI and demographic model	74 (63–83)	66 (57–75)	61 (50–71)	79 (69–86)	2.20	<0.0001
IPAH, prognostic model 3 yr						
RV end-systolic volume %pred	72 (55–86)	64 (53–74)	46 (32–59)	85 (74–93)	2.00	0.0003
MRI model	83 (67–94)	63 (52–73)	49 (36–61)	90 (79–96)	2.24	<0.0001
MRI and demographic model	89 (74–97)	76 (65–84)	60 (46–74)	94 (85–98)	3.64	<0.0001

Definition of abbreviations: IPAH = idiopathic pulmonary arterial hypertension; LHR = likelihood ratio; MRI = magnetic resonance imaging; NPV = negative predictive value; PAH = pulmonary arterial hypertension; PPV = positive predictive value; RV = right ventricular; Sens = sensitivity; Spec = specificity. Data in parentheses are 95% confidence intervals. The MRI model and MRI and demographic model were generated in the derivation cohort. For each variable, optimal thresholds were identified in the derivation cohort. Thresholds identified in the derivation cohort are as follows: RV end-systolic volume (225), MRI model (0.13), MRI and demographic model (2.9).

noninvasive PA relative area change and PA distensibility, and no significant difference at ROC analysis between the two measures. This may reflect the close correlation between these two metrics ($r = 0.88$).

Patient age has been shown to strongly predict mortality in several PAH cohorts (39, 40). These studies have also demonstrated that the range and average age of patients has risen significantly over the last decade making adjustments for age and sex more relevant in the current era for accurate individual risk stratification (41). RVESV corrected for age, sex and body surface was a significantly stronger predictor of mortality than when adjusted for body surface area alone, highlighting the need to adjust volumetric measurements for individual patients. We have corrected our data using data by Maceira et al (33) due to similarity in RV analysis technique for the main analyses, however, other normative RV data, such as Kawut et al (34), is available and demonstrated similar prognostic value in our cohort of patients. In the present study RVESVI %pred rather than RVEDV %pred was independently prognostic; increased RVESV implies enlargement of the RV in addition to a loss of systolic function and may explain the greater prognostic importance. This finding mirrors data in chronic heart failure, in which increasing RVESV has been shown to be an independent predictor of mortality (42).

In the present study patients on monotherapy with a phosphodiesterase inhibitor or endothelin receptor antagonist had a worse outcome than patients on a phosphodiesterase inhibitor and endothelin receptor antagonist in combination, with the patients in this study receiving sequential rather than upfront combination. Although this is a retrospective study, it is consistent with a prospective double-blinded study, which showed the benefit of sequential combination therapy over monotherapy in patients with PAH (43) in reducing clinical worsening and a MRI focused study of up front combination therapy in systemic sclerosis which demonstrated improvements in RV function (44). Despite improved outcomes PAH remains a life shortening condition and identification of reproducible and prognostic end-points in PAH will help to assess the value of new therapeutic agents (45).

In clinical practice, assessments are based on integrating available information and there has been a move toward developing scoring systems to aid prognostication. ROC curves are frequently used to assess the value of diagnostic tests, however, there is only limited data on assessing the prognostic value of candidate prognostic markers in PAH using ROC analysis. The prognostic value of a single MRI measurement was improved by combining MRI metrics and further improved by incorporating additional clinical data, obtaining ROC values equal to or better than previous studies in cardiac disease that estimate cardiovascular risk (46). However, the value of predictive models depends on the clinical context. In PAH high levels of predictive accuracy are required when deciding on lung transplant or commencing IV prostanoid therapy and this is more immediately critical than deciding whether or not to give statins or lifestyle advice. In the present study MRI has shown similar prognostic accuracy to baseline 6-minute-walk test (AUC, 0.74) (47).

Limitations

This is a single center study. Race has been shown to have an independent effect on RV volumes; however, the demographic of our population does not allow direct comparison with the published reference data (34) and we have not adjusted MRI data for race in this study. There is limited normative data on pulmonary vascular measurements such as PA relative area change, further work in this area is warranted to determine the influence of age, race and sex. This study shows that individual MRI metrics have limitations when used in the prognostic assessment of patients with PAH. Though improved accuracy can be achieved by combining MRI metrics with clinical data the PPV and NPV highlight that there are uncertainties in how best to use this investigation in the pulmonary hypertension clinic. MRI does have limitations including claustrophobia, pacemaker and metallic foreign bodies precluding in its use in approximately 5% of pulmonary hypertension cases (17). Compared with other investigations such as the 6-minute-walk test it is more expensive and time consuming to perform and availability is more limited. Nonetheless the higher reproducibility of CMR compared

with other biomarkers and the multiple quantitative measurements, that can be made that relate to disease severity, suggest utility in the follow-up of patients with PAH. Given that prognosis is dependent on the severity of disease at the time of evaluation and response to treatment further study of the value of follow-up imaging in large cohorts of patients is warranted.

Conclusions

MRI measurements of RV structure and function are highly reproducible and have prognostic value. Combining MRI measures of RV function and PA stiffness with clinical data further improves prognostication in patients with PAH. Further work evaluating the role of MRI in the pulmonary hypertension clinic is warranted. ■

Author disclosures are available with the text of this article at www.atsjournals.org.

References

1. Galie N, Humbert M, Vachiery JL, Gibbs S, Lang I, Torbicki A, Simonneau G, Peacock A, Vonk Noordegraaf A, Beghetti M, *et al*. 2015 ESC/ERS guidelines for the diagnosis and treatment of pulmonary hypertension: the Joint Task Force for the Diagnosis and Treatment of Pulmonary Hypertension of the European Society of Cardiology (ESC) and the European Respiratory Society (ERS) Endorsed by: Association for European Paediatric and Congenital Cardiology (AEPC), International Society for Heart and Lung Transplantation (ISHLT). *Eur Heart J* 2016;37:67–119.
2. Kiely DG, Elliot CA, Sabroe I, Condliffe R. Pulmonary hypertension: diagnosis and management. *BMJ* 2013;346:f2028.
3. Benza RL, Miller DP, Gomberg-Maitland M, Frantz RP, Foreman AJ, Coffey CS, Frost A, Barst RJ, Badesch DB, Elliott CG, *et al*. Predicting survival in pulmonary arterial hypertension: insights from the Registry to Evaluate Early and Long-Term Pulmonary Arterial Hypertension Disease Management (REVEAL). *Circulation* 2010; 122:164–172.
4. D'Alonzo GE, Barst RJ, Ayres SM, Bergofsky EH, Brundage BH, Detre KM, Fishman AP, Goldring RM, Groves BM, Kernis JT, *et al*. Survival in patients with primary pulmonary hypertension. Results from a national prospective registry. *Ann Intern Med* 1991;115:343–349.
5. Nickel N, Golpon H, Greer M, Knudsen L, Olsson K, Westerkamp V, Welte T, Hoeper MM. The prognostic impact of follow-up assessments in patients with idiopathic pulmonary arterial hypertension. *Eur Respir J* 2012;39:589–596.
6. Humbert M, Sitbon O, Chaouat A, Bertocchi M, Habib G, Gressin V, Yaïci A, Weitzenblum E, Cordier JF, Chabot F, *et al*. Survival in patients with idiopathic, familial, and anorexigen-associated pulmonary arterial hypertension in the modern management era. *Circulation* 2010;122: 156–163.
7. Wensel R, Francis DP, Meyer FJ, Opitz CF, Bruch L, Halank M, Winkler J, Seyfarth HJ, Gläser S, Blumberg F, *et al*. Incremental prognostic value of cardiopulmonary exercise testing and resting haemodynamics in pulmonary arterial hypertension. *Int J Cardiol* 2013;167: 1193–1198.
8. Sandoval J, Bauerle O, Palomar A, Gómez A, Martínez-Guerra ML, Beltrán M, Guerrero ML. Survival in primary pulmonary hypertension. Validation of a prognostic equation. *Circulation* 1994; 89:1733–1744.
9. Sitbon O, Benza RL, Badesch DB, Barst RJ, Elliott CG, Gressin V, Lemarié JC, Miller DP, Muros-Le Rouzic E, Simonneau G, *et al*. Validation of two predictive models for survival in pulmonary arterial hypertension. *Eur Respir J* 2015;46:152–164.
10. Grothues F, Moon JC, Bellenger NG, Smith GS, Klein HU, Pennell DJ. Interstudy reproducibility of right ventricular volumes, function, and mass with cardiovascular magnetic resonance. *Am Heart J* 2004; 147:218–223.
11. Grothues F, Smith GC, Moon JC, Bellenger NG, Collins P, Klein HU, Pennell DJ. Comparison of interstudy reproducibility of cardiovascular magnetic resonance with two-dimensional echocardiography in normal subjects and in patients with heart failure or left ventricular hypertrophy. *Am J Cardiol* 2002;90:29–34.
12. Mooij CF, de Wit CJ, Graham DA, Powell AJ, Geva T. Reproducibility of MRI measurements of right ventricular size and function in patients with normal and dilated ventricles. *J Magn Reson Imaging* 2008;28: 67–73.
13. Gan CT, Lankhaar JW, Westerhof N, Marcus JT, Becker A, Twisk JW, Boonstra A, Postmus PE, Vonk-Noordegraaf A. Noninvasively assessed pulmonary artery stiffness predicts mortality in pulmonary arterial hypertension. *Chest* 2007;132:1906–1912.
14. Sanz J, Kariisa M, Dellegrottaglie S, Prat-González S, Garcia MJ, Fuster V, Rajagopalan S. Evaluation of pulmonary artery stiffness in pulmonary hypertension with cardiac magnetic resonance. *JACC Cardiovasc Imaging* 2009;2:286–295.
15. Sanz J, Kuschnir P, Rius T, Salguero R, Sulica R, Einstein AJ, Dellegrottaglie S, Fuster V, Rajagopalan S, Poon M. Pulmonary arterial hypertension: noninvasive detection with phase-contrast MR imaging. *Radiology* 2007;243:70–79.
16. Swift AJ, Rajaram S, Condliffe R, Capener D, Hurdman J, Elliot C, Kiely DG, Wild JM. Pulmonary artery relative area change detects mild elevations in pulmonary vascular resistance and predicts adverse outcome in pulmonary hypertension. *Invest Radiol* 2012;47: 571–577.
17. Swift AJ, Rajaram S, Condliffe R, Capener D, Hurdman J, Elliot CA, Wild JM, Kiely DG. Diagnostic accuracy of cardiovascular magnetic resonance imaging of right ventricular morphology and function in the assessment of suspected pulmonary hypertension results from the ASPIRE registry. J Cardiovasc Magn Reson 2012;14:40.
18. Saba TS, Foster J, Cockburn M, Cowan M, Peacock AJ. Ventricular mass index using magnetic resonance imaging accurately estimates pulmonary artery pressure. *Eur Respir J* 2002;20: 1519–1524.
19. Alunni JP, Degano B, Arnaud C, Tétu L, Blot-Soulétie N, Didier A, Otal P, Rousseau H, Chabbert V. Cardiac MRI in pulmonary artery hypertension: correlations between morphological and functional parameters and invasive measurements. *Eur Radiol* 2010;20: 1149–1159.
20. Reiter G, Reiter U, Kovacs G, Kainz B, Schmidt K, Maier R, Olschewski H, Rienmueller R. Magnetic resonance-derived 3-dimensional blood flow patterns in the main pulmonary artery as a marker of pulmonary hypertension and a measure of elevated mean pulmonary arterial pressure. *Circ Cardiovasc Imaging* 2008;1:23–30.
21. Lungu A, Wild JM, Capener D, Kiely DG, Swift AJ, Hose DR. MRI model-based non-invasive differential diagnosis in pulmonary hypertension. *J Biomech* 2014;47:2941–2947.
22. van Wolferen SA, Marcus JT, Boonstra A, Marques KM, Bronzwaer JG, Spreeuwenberg MD, Postmus PE, Vonk-Noordegraaf A. Prognostic value of right ventricular mass, volume, and function in idiopathic pulmonary arterial hypertension. *Eur Heart J* 2007;28: 1250–1257.
23. van de Veerdonk MC, Kind T, Marcus JT, Mauritz GJ, Heymans MW, Bogaard HJ, Boonstra A, Marques KM, Westerhof N, Vonk-Noordegraaf A. Progressive right ventricular dysfunction in patients with pulmonary arterial hypertension responding to therapy. *J Am Coll Cardiol* 2011;58:2511–2519.
24. Vanderpool RR, Pinsky MR, Naeije R, Deible C, Kosaraju V, Bunner C, Mathier MA, Lacomis J, Champion HC, Simon MA. RV-pulmonary arterial coupling predicts outcome in patients referred for pulmonary hypertension. *Heart* 2015;101:37–43.
25. Swift AJ, Rajaram S, Campbell MJ, Hurdman J, Thomas S, Capener D, Elliot C, Condliffe R, Wild JM, Kiely DG. Prognostic value of cardiovascular magnetic resonance imaging measurements corrected for age and sex in idiopathic pulmonary arterial hypertension. *Circ Cardiovasc Imaging* 2014;7:100–106.

26. Hurdman J, Condliffe R, Elliot CA, Davies C, Hill C, Wild JM, Capener D, Sephton P, Hamilton N, Armstrong IJ, *et al*. ASPIRE registry: assessing the spectrum of pulmonary hypertension identified at a REferral centre. *Eur Respir J* 2012;39:945–955.
27. Mauritz GJ, Marcus JT, Boonstra A, Postmus PE, Westerhof N, Vonk-Noordegraaf A. Non-invasive stroke volume assessment in patients with pulmonary arterial hypertension: left-sided data mandatory. *J Cardiovasc Magn Reson* 2008;10:51.
28. Toshner MR, Gopalan D, Suntharalingam J, Treacy C, Soon E, Sheares KK, Morrell NW, Screaton N, Pepke-Zaba J. Pulmonary arterial size and response to sildenafil in chronic thromboembolic pulmonary hypertension. *J Heart Lung Transplant* 2010;29:610–615.
29. Galiè N, Hoeper MM, Humbert M, Torbicki A, Vachiery JL, Barbera JA, Beghetti M, Corris P, Gaine S, Gibbs JS, *et al*.; ESC Committee for Practice Guidelines (CPG). Guidelines for the diagnosis and treatment of pulmonary hypertension: the Task Force for the Diagnosis and Treatment of Pulmonary Hypertension of the European Society of Cardiology (ESC) and the European Respiratory Society (ERS), endorsed by the International Society of Heart and Lung Transplantation (ISHLT). *Eur Heart J* 2009;30:2493–2537.
30. Sanz J, García-Alvarez A, Fernández-Friera L, Nair A, Mirelis JG, Sawit ST, Pinney S, Fuster V. Right ventriculo-arterial coupling in pulmonary hypertension: a magnetic resonance study. *Heart* 2012;98:238–243.
31. Wong RC, Dumont CA, Austin BA, Kwon DH, Flamm SD, Thomas JD, Starling RC, Desai MY. Relation of ventricular-vascular coupling to exercise capacity in ischemic cardiomyopathy: a cardiac multi-modality imaging study. *Int J Cardiovasc Imaging* 2010;26:151–159.
32. Najjar SS, Schulman SP, Gerstenblith G, Fleg JL, Kass DA, O'Connor F, Becker LC, Lakatta EG. Age and gender affect ventricular-vascular coupling during aerobic exercise. *J Am Coll Cardiol* 2004;44:611–617.
33. Maceira AM, Prasad SK, Khan M, Pennell DJ. Reference right ventricular systolic and diastolic function normalized to age, gender and body surface area from steady-state free precession cardiovascular magnetic resonance. *Eur Heart J* 2006;27:2879–2888.
34. Kawut SM, Lima JA, Barr RG, Chahal H, Jain A, Tandri H, Praestgaard A, Bagiella E, Kizer JR, Johnson WC, *et al*. Sex and race differences in right ventricular structure and function: the multi-ethnic study of atherosclerosis-right ventricle study. *Circulation* 2011;123: 2542–2551.
35. Hanley JA, McNeil BJ. The meaning and use of the area under a receiver operating characteristic (ROC) curve. *Radiology* 1982;143: 29–36.
36. Vonk-Noordegraaf A, Haddad F, Chin KM, Forfia PR, Kawut SM, Lumens J, Naeije R, Newman J, Oudiz RJ, Provencher S, *et al*. Right heart adaptation to pulmonary arterial hypertension: physiology and pathobiology. *J Am Coll Cardiol* 2013;62(Suppl 25):D22–D33.
37. Trip P, Kind T, van de Veerdonk MC, Marcus JT, de Man FS, Westerhof N, Vonk-Noordegraaf A. Accurate assessment of load-independent right ventricular systolic function in patients with pulmonary hypertension. *J Heart Lung Transplant* 2013;32:50–55.
38. Tedford RJ, Mudd JO, Girgis RE, Mathai SC, Zaiman AL, Housten-Harris T, Boyce D, Kelemen BW, Bacher AC, Shah AA, *et al*. Right ventricular dysfunction in systemic sclerosis-associated pulmonary arterial hypertension. *Circ Heart Fail* 2013;6: 953–963.
39. Benza RL, Gomberg-Maitland M, Miller DP, Frost A, Frantz RP, Foreman AJ, Badesch DB, McGoon MD. The REVEAL Registry risk score calculator in patients newly diagnosed with pulmonary arterial hypertension. *Chest* 2012;141:354–362.
40. Ling Y, Johnson MK, Kiely DG, Condliffe R, Elliot CA, Gibbs JS, Howard LS, Pepke-Zaba J, Sheares KK, Corris PA, *et al*. Changing demographics, epidemiology, and survival of incident pulmonary arterial hypertension: results from the pulmonary hypertension registry of the United Kingdom and Ireland. *Am J Respir Crit Care Med* 2012;186:790–796.
41. Lee WT, Ling Y, Sheares KK, Pepke-Zaba J, Peacock AJ, Johnson MK. Predicting survival in pulmonary arterial hypertension in the UK. *Eur Respir J* 2012;40:604–611.
42. Bourantas CV, Loh HP, Bragadeesh T, Rigby AS, Lukaschuk EI, Garg S, Tweddel AC, Alamgir FM, Nikitin NP, Clark AL, *et al*. Relationship between right ventricular volumes measured by cardiac magnetic resonance imaging and prognosis in patients with chronic heart failure. *Eur J Heart Fail* 2011;13:52–60.
43. Pulido T, Adzerikho I, Channick RN, Delcroix M, Galiè N, Ghofrani HA, Jansa P, Jing ZC, Le Brun FO, Mehta S, *et al*.; SERAPHIN Investigators. Macitentan and morbidity and mortality in pulmonary arterial hypertension. *N Engl J Med* 2013;369:809–818.
44. Hassoun PM, Zamanian RT, Damico R, Lechtzin N, Khair R, Kolb TM, Tedford RJ, Hulme OL, Housten T, Pisanello C, *et al*. Ambrisentan and tadalafil up-front combination therapy in scleroderma-associated pulmonary arterial hypertension. *Am J Respir Crit Care Med* 2015;192:1102–1110.
45. Chun HJ, Bonnet S, Chan SY. Translational advances in the field of pulmonary hypertension. Translating microRNA biology in pulmonary hypertension. it will take more than "miR" words. *Am J Respir Crit Care Med* 2017;195:167–178.
46. Siontis GC, Tzoulaki I, Siontis KC, Ioannidis JP. Comparisons of established risk prediction models for cardiovascular disease: systematic review. *BMJ* 2012;344:e3318.
47. Lee WT, Peacock AJ, Johnson MK. The role of per cent predicted 6-min walk distance in pulmonary arterial hypertension. *Eur Respir J* 2010;36:1294–1301.